



**Relative Anion Stabilities and Transition State Energies Regarding Vinylic vs Allylic Deprotonation of Cyclic Vinyl Ethers by Organolithium Reagents:  
An *Ab Initio* Study**

Trevor D. Power and John F. Sebastian\*

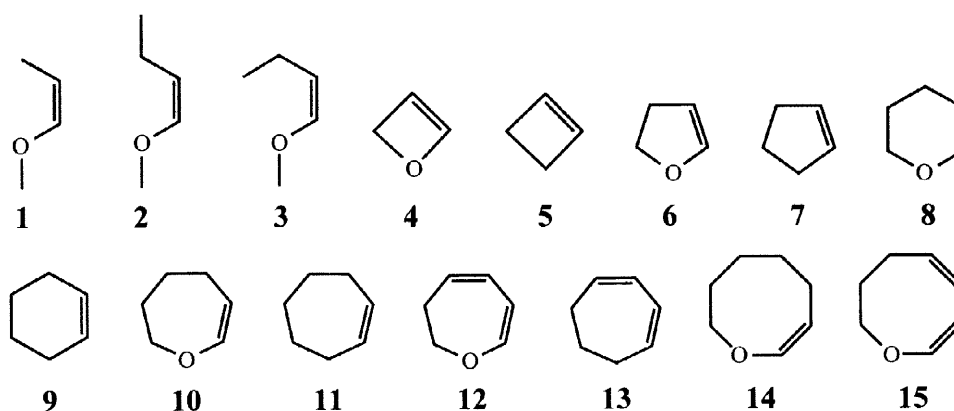
Miami University, Department of Chemistry and Biochemistry, Oxford, Ohio 45056 USA

Received 4 November 1997; revised 4 May 1998; accepted 5 May 1998

**Abstract:** The relative energies of allylic and vinylic anions of several vinyl ethers were determined by *ab initio* calculations at the Hartree-Fock and second-order Møller-Plesset perturbation theory (single point) levels using basis set 6-31++G(d,p) in an attempt at explaining experimental results concerning allylic vs vinylic deprotonation. A general trend with cyclic vinyl ethers has been discovered where the stability of the allyl anion over the vinyl anion in terms of ring size is  $8 \approx 7 > 6 > 5 \approx 4$ . In general, optimized vinyl anions exhibit a vinyl angle compression whereas optimized allyl anions exhibit an allyl angle expansion. Additionally, transition state structures are examined that invoke a pre-equilibrium complexation of lithium to the electron rich vinyl ether oxygens prior to the formation of the deprotonation products. These transition states are suggestive of multi-center processes, precluding the formation of free ions during these deprotonation reactions. In many cases, the stabilization energy of the appropriate transition state is in agreement with the experimentally observed product. © 1998 Elsevier Science Ltd. All rights reserved.

Experimentally, it has been shown that 2,3-dihydrofuran (**6**), 2,3-dihydro-4H-pyran (**8**), and 2,3,4,5-tetrahydrooxepin (**10**) react with alkyl lithium reagents to form vinyl lithiated species.<sup>1,2</sup> Under the same

Chart I. Structures



reaction conditions, 2,3-dihydrooxepin (**12**) forms 1-lithio-1-oxaheptatriene,<sup>2</sup> a product that may have arisen through the intermediacy of the corresponding allylic anion. Alternatively, the vinyl anion of 2,3-

dihydrooxepin may form and react with a second molecule of 2,3-dihydrooxepin and deprotonate the allylic position. As the relative stabilities of the vinylic and allylic anions of these compounds had never been examined previously,<sup>3</sup> it was left to speculate how these products form. In order to better understand allylic vs. vinylic deprotonation, *ab initio* calculations were used to examine **6**, **8**, **10**, **12**, (Z)-1-propenyl methyl ether (**1**), *anti*-(Z)-1-butenyl methyl ether (**2**), *syn*-(Z)-1-butenyl methyl ether (**3**), oxete (**4**), cyclobutene (**5**), cyclopentene (**7**), cyclohexene (**9**), cycloheptene (**11**), 1,3-cycloheptadiene (**13**), 2,3,5,6-tetrahydro-4H-oxocin (**14**), and 2,3-dihydro-4H-oxocin (**15**) in an attempt to explore 1) relative anion stability, 2) the effect ring size has on the site of deprotonation.

There is significant evidence pertaining to metalation of compounds containing electron rich atoms with some alkyl lithium reagents, suggestive of complexation between lithium and these electronegative sites prior to formation of the experimentally observed product.<sup>4-7</sup> In cases where the experimentally observed product(s) is/are described as being unexpected due to thermodynamic or kinetic considerations, this complexation has been termed the Complex Induced Proximity Effect (CIPE) by Beak et al.<sup>8,9</sup> In all of these cases, lithium selectively delivers the appropriate carbanion to a specific site in the substrate. Deprotonation of vinyl ethers may proceed through an analogous process, albeit not CIPE mediated for most cases where experimental data are currently available. A possible exception is 2,3-dihydrooxepin where deprotonation of the most acidic (vinyl) proton is not observed and this may occur via CIPE. It is therefore important to examine the transition states corresponding to vinylic and allylic deprotonation.

## COMPUTATIONAL DETAILS

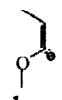
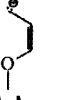
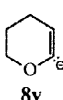
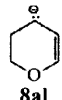
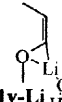
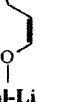
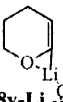
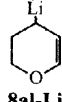
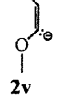
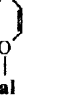
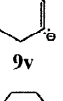
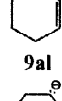
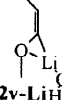
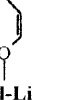
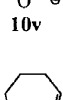
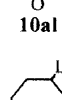
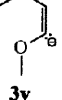
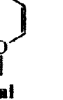
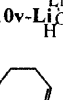
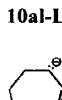
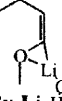
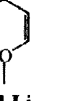


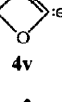
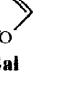


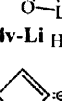

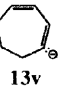
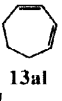
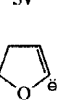
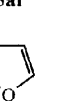
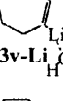
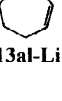
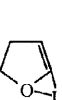
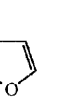
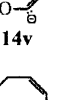
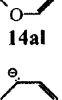
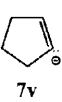
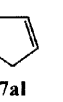
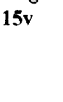
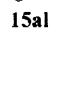




*Ab initio* calculations were performed using Gaussian 94.<sup>10</sup> Geometry optimizations were completed on structures shown in Chart 1, Table 1, Figures 1-5 at the Restricted Hartree-Fock (RHF) level of theory using the 6-31++G(d,p) basis set. Transition states **8v-ts** and **8al-ts** were additionally optimized at the RHF level using basis set 6-311++G(d,p). Concerning transition states **10v-ts** and **10al-ts**, we also performed optimizations with basis sets aug-cc-pVDZ (H, C, O)<sup>11-15</sup> and 6-31G (Li) at the RHF level of theory. Furthermore, for these optimized geometries we present single point energy calculations obtained from frozen core second-order Møller Plesset perturbation theory (MP2-FC). For transition states **8v-ts**, **8al-ts**, **10v-ts**, and **10al-ts** we present energies obtained employing single point B3LYP<sup>16-19</sup> calculations of these optimized geometries requesting the full SCF convergence criterion (SCF=Tight). Each stationary point was verified as a minimum or transition state using analytical second derivative vibrational frequency calculations.

## RESULTS AND DISCUSSION

**Vinyl and allyl anions.** *Ab initio* calculations predict (Table 1) that the vinyl anions (**2v**, **3v**, **4v**, **5v**, and **6v**) are more stable than the corresponding allyl anions (**2al**, **3al**, **4al**, **5al**, and **6al**) by about 3, 3, 14, 5, and 11 kcal/mol (RHF) respectively and in the case of **4v** and **6v** vs **4al** and **6al**, 4 and 6 kcal/mol (MP2) respectively. Results at the MP2 level of theory for **2v** vs. **2al** and **3v** vs. **3al** do not significantly favor the stability of either anion. MP2 single point calculations indicate that the allylic anion **5al** is lower in energy than the vinylic anion **5v** by about 3 kcal/mol; a result opposite to that obtained at the Hartree-Fock level of theory for these anions. Allyl anions (**1al**, **7al**, **8al**, **9al**, **10al**, **11al**, **12al**, **13al**, **14al**, and **15al**) are predicted to be more stable than the corresponding vinyl anions (**1v**, **7v**, **8v**, **9v**, **10v**, **11v**, **12v**, **13v**, **14v**, and **15v**) by about 1, 4, 1, 11, 5, 16, 15, 25, 5 and 15 kcal/mol (RHF) and 4, 11, 6, 15, 10, 21, 22, 31, 8, and 19 kcal/mol (MP2) respectively. The relative energies for **14v** vs **14al** are calculated by comparison of the lowest energy boat conformation of **14v** against the lowest energy chair conformation of **14al** (see Figure 1). Due to the insignificant differences in relative energies for **1v** vs. **1al** and **8v** vs. **8al** at the Hartree-Fock level of theory, the MP2 results serve to assist in defining the allyl anions as the lower energy species. (Refer to Figures 1, 2 for optimized structures and relative energies for “boat” and “chair” conformations of (**14**, **14v**, and **14al**) and (**15**, **15v**, and **15al**) respectively.) Optimized local minima **3** and **3v** are first order saddle points and additionally, **3al** is a second order saddle point. Results for vinyl lithiated species **3v-Li** correspond to a *partial* optimization performed by restricting the dihedral angle containing the four 1-butenyl carbon atoms to 0.000° and is *not* a stationary point. In order to locate an energy well that satisfies the default force and displacement convergence criteria set in Gaussian 94, this dihedral was moved to 0.012°. Subsequent attempts at optimizing the geometry of **3v-Li** without geometry constraints led to the *anti* conformation (**2v-Li**). No symmetry constraints were employed during the geometry optimizations shown in Table 1. In every case, employing symmetry constraints results in an extrema that is either essentially equivalent or greater in energy to that obtained without enforcing symmetry constraints and some of these higher energy extrema are not zeroth-order.

To the best of our knowledge, experimental data concerning the gas-phase geometries of the vinyl ethers are unavailable in the literature at this time. With regard to the cycloalkenes (**5**<sup>20-21</sup>, **7**<sup>22</sup>, **9**<sup>23</sup>, **11**<sup>24</sup>, and **13**<sup>25</sup>), experimental structural data are available. Optimizations at the Hartree-Fock level of theory in the 6-31++G(d,p) basis set give very similar results compared to those obtained experimentally. For the vinyl ethers, the degree of accuracy concerning gas-phase geometries, determined by RHF/6-31++G(d,p) optimizations, is unknown, but is expected to be similar to that of cyclic alkenes.

Table 1. Relative Energies (kcal/mol) using Basis Set 6-31++G(d,p)  
(lowest energy species assigned a value of 0.00 kcal/mol)

	HF	MP2 Single Point		HF	MP2 Single Point		HF	MP2 Single Point		HF	MP2 Single Point
	1.20	3.60		0.00	0.00		0.69	5.86		0.00	0.00
	8.19	11.0		0.00	0.00		0.00	0.00		10.9	7.00
	0.00	0.43		3.26	0.00		11.2	15.3		0.00	0.00
	4.95	8.57		0.00	0.00		5.49	10.0		0.00	0.00
	0.00	0.90		2.55	0.00		0.00	5.10		0.92	0.00
	6.15	10.4		0.00	0.00		15.8	20.6		0.00	0.00
	0.00	0.00		13.6	4.32		15.2	22.1		0.00	0.00
	0.00	0.00		7.44	2.14		10.8	20.1		0.00	0.00
	0.00	3.12		4.94	0.00		24.9	30.9		0.00	0.00
	0.00	0.00		10.8	5.53		17.0	27.8		0.00	0.00
	0.00	0.00		10.0	2.98		Boat 4.58	7.54		Chair 0.00	0.00
	4.04	10.6		0.00	0.00		Boat 14.4	19.3		Boat 0.00	0.00
							Chair 15.3	18.0		Chair 0.00	0.00

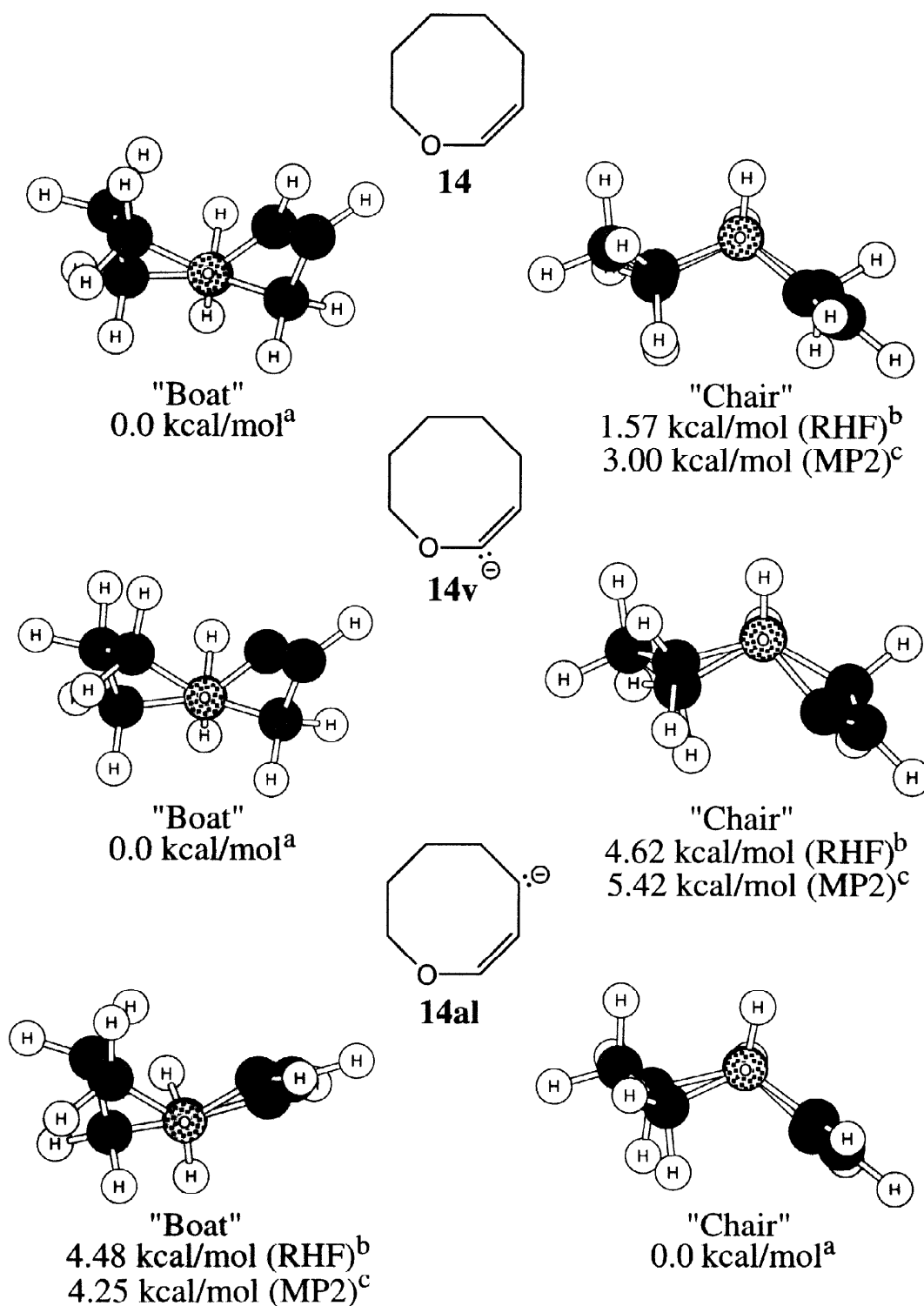


Figure 1. Optimized Geometries of and Relative Energies Between the "Chair" and "Boat" Conformations of **14**, **14v**, and **14al** (lowest energy species assigned a value of 0.0 kcal/mol)

<sup>a</sup> Lowest Energy Conformer at both Hartree-Fock and MP2 levels of theory. <sup>b</sup> Relative Hartree-Fock energy obtained from RHF/6-31++G(d,p) optimization. <sup>c</sup> Relative energy from MP2/6-31++G(d,p)/RHF/6-31++G(d,p)

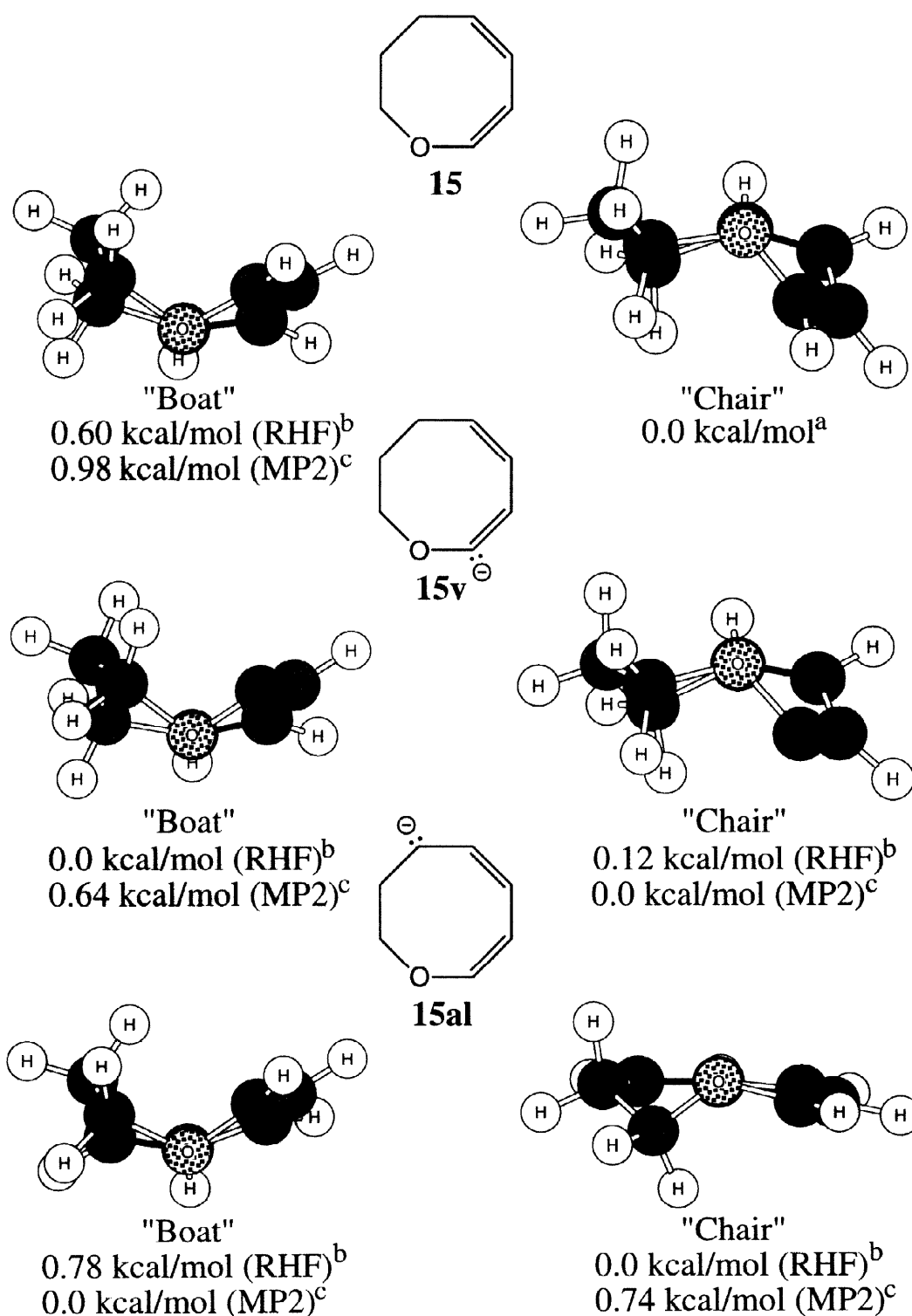


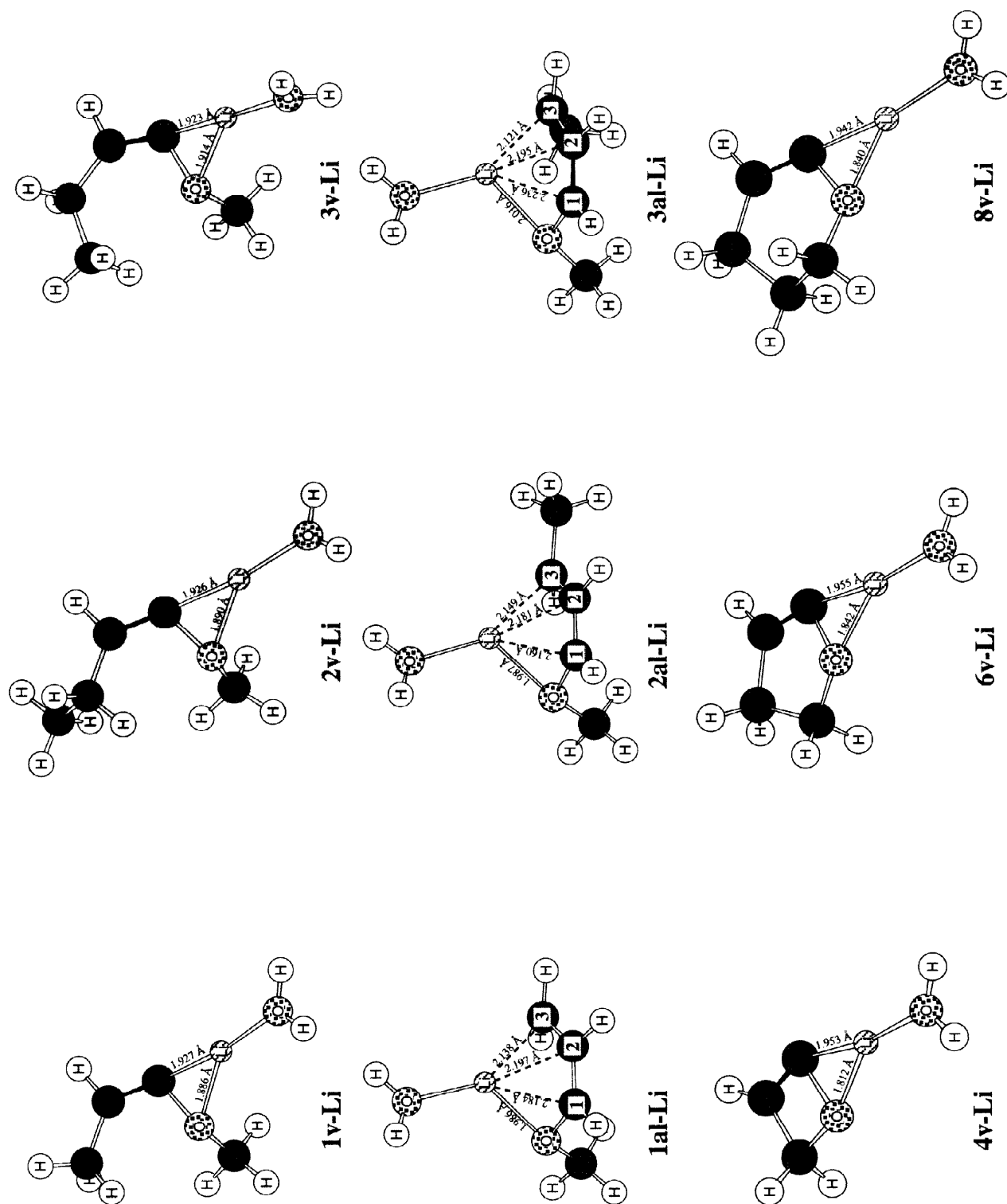
Figure 2. Optimized Geometries of and Relative Energies Between the "Chair" and "Boat" Conformations of **15**, **15v**, and **15al** (lowest energy species assigned a value of 0.0 kcal/mol)

<sup>a</sup> Lowest Energy Conformer at both Hartree-Fock and MP2 levels of theory. <sup>b</sup> Relative Hartree-Fock energy obtained from RHF/6-31++G(d,p) optimization. <sup>c</sup> Relative energy from MP2/6-31++G(d,p)/RHF/6-31++G(d,p)

A general trend can be noted concerning the relative stabilities of the cyclic vinyl ether anions such that the relative stability of the allylic anions over the vinylic anions in terms of ring size is  $8 \approx 7 > 6 > 5 \approx 4$  where, again, in the case of the 4 and 5-membered ring, the vinyl anions (**4v** and **6v**) are stabilized over the corresponding allylic anions **4al** and **6al**. The 7-membered ring pentadienyl anion **12al** is stabilized over **12v** more than the 7-membered ring allyl anion **10al** is over **10v**. Analogously, the 8-membered ring pentadienyl anion **15al** is lower in energy than the corresponding vinylic anion **15v** and this relative energy difference is greater than that between the 8-membered ring allylic anion **14al** and the higher energy vinylic anion **14v**. With regard to the cyclic vinyl hydrocarbons, the stability trend of the allylic anions over the vinylic anions in terms of ring size is  $7 > 6 > 5 > 4$ . Also, as was seen in the cyclic vinyl ethers, comparison of the relative energies corresponding to the pentadienyl anion **13al** and the vinyl anion **13v** indicate that **13al** is lower in energy and this difference is significantly greater than the relative energy between the more stable allyl anion **11al** as compared to the vinyl anion **11v**. The relative stabilities of the lithiated species are also presented in Table 1.

**Solvated vinyl and allyl lithiated species.** Coordination of lithium with a water molecule is being used as a model for ether solvation. The vinyl lithiated species (**4v-Li**, **6v-Li**, **8v-Li**, and **10v-Li**) are predicted to be about 7, 10, 11 and 1 kcal/mol (RHF) more stable than the corresponding allyl lithiated species (**4al-Li**, **6al-Li**, **8al-Li** and **10al-Li**). MP2 results suggest that the vinyl lithiated species (**4v-Li**, **6v-Li**, and **8v-Li**) are more stable than the corresponding allyl lithiated species (**4al-Li**, **6al-Li**, and **8al-Li**) by about 2, 3, and 7 kcal/mol respectively. MP2 results for **10v-Li** vs **10al-Li** suggest that the allyl lithiated species **10al-Li** is about 5 kcal/mol lower in energy than the corresponding vinyl lithiated species **10v-Li**. In spite of the fact that the allyl anion **8al** is predicted to be lower in energy than the vinyl anion **8v**, the vinyl lithiated species **8v-Li** is lower in energy than the allyl lithiated species **8al-Li**. Thus, the reaction responsible for the formation of the vinyl lithiated species may be driven by product stability rather than anion stability. Nevertheless, this cannot explain the experimentally observed vinyl lithiated species **10v-Li** vs. the allyl lithiated species **10al-Li** which is predicted to be lower in energy than **10v-Li** at the MP2 level of theory. The allyl lithiated species (**1al-Li**, **2al-Li**, **3al-Li**, **12al-Li**, and **13al-Li**) are predicted to be about 8, 5, 6, 11, and 17 kcal/mol (RHF) and 11, 9, 10, 20, and 28 kcal/mol (MP2) lower in energy than the corresponding vinyl lithiated species (**1v-Li**, **2v-Li**, **3v-Li**, **12v-Li**, and **13v-Li**). Both the lower energy allyl anion **12al** and the lower energy allyl lithiated species **12al-Li** are consistent with the idea of allylic deprotonation of **12** to give **12al-Li** subsequently yielding 1-lithio-1-oxaheptatriene.<sup>2</sup>

**Solvated Structures.** Geometries for the water solvated vinyl and allyl lithiated species (**1v-Li**, **1al-**





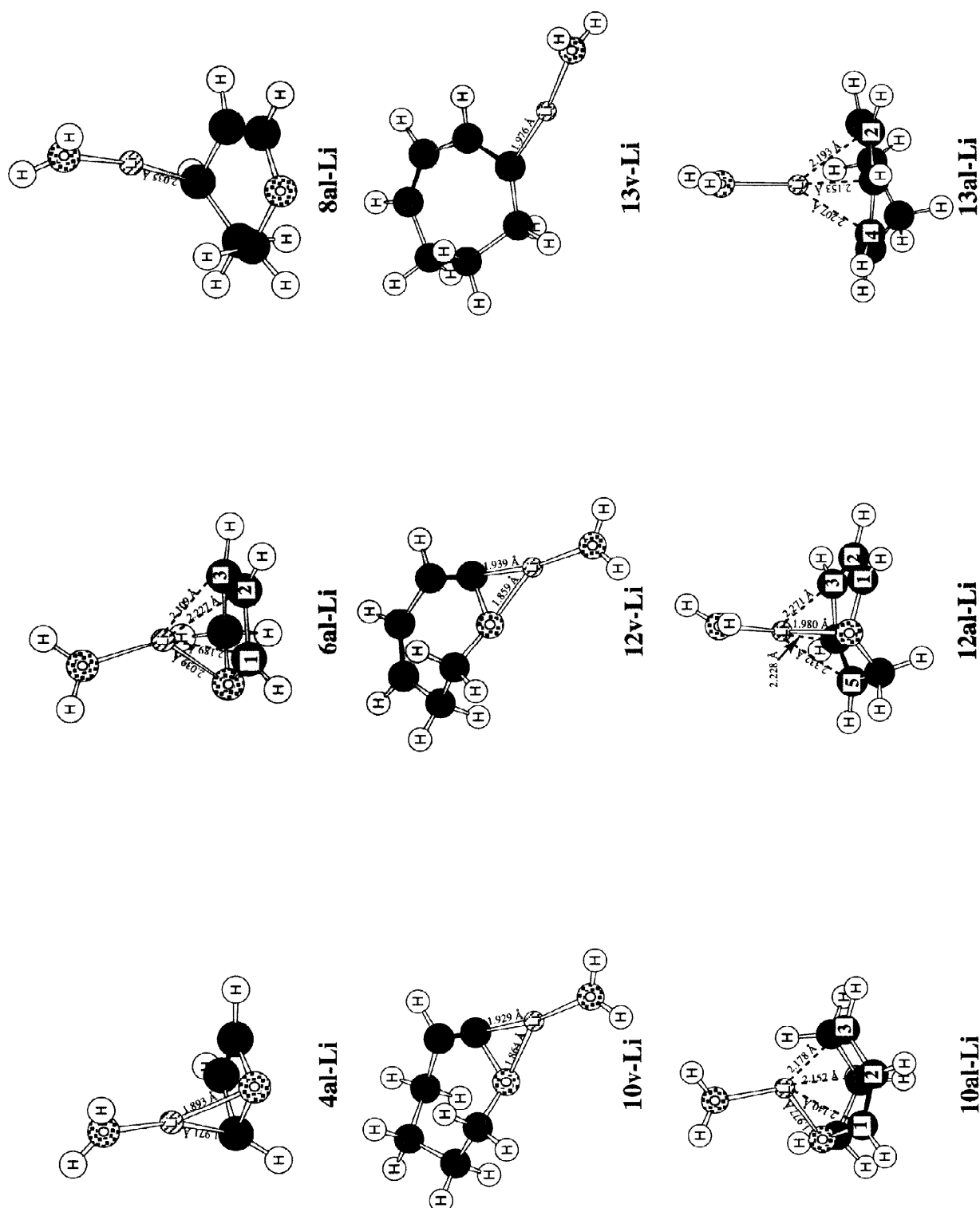


Figure 3. Chem 3-D Plots of Optimized Solvated Structures Obtained From RHF/6-31++G(d,p) Optimization

**12al-Li**, **13v-Li**, **13al-Li**) obtained at the Hartree-Fock level of theory with the 6-31++G(d,p) basis set are presented in Figure 3 along with explicit bond lengths (in Å) of the solvated lithium coordination. In all of the cases involving vinyl lithiation of cyclic vinyl ethers, the optimized geometries of the lithiated vinyl ethers, consistent with previously published data<sup>4</sup>, demonstrate solvated lithium coordinating to not only the vinyl carbon (site of deprotonation), but additionally the adjacent ether oxygen, forming a three-membered ring. In order to better understand the geometries obtained for the allyl lithiated species, the charges from a Natural Population Analysis<sup>26-27</sup> (NPA) and the molecular orbital coefficients of the HOMOs (Highest Occupied Molecular Orbitals) were calculated for the optimized geometries of the corresponding allyl anions from the electron density at the MP2 level of theory (Density=MP2). The position of the lithium atom in the geometries obtained for **1al-Li**, **2al-Li**, and **6al-Li** shows complexation to the two terminal carbons of the allylic system, labeled **1** and **3** in Figure 3, (as well as complexation to the ether oxygen) and this is consistent with the much larger size of the p-orbitals of the HOMO. The ether oxygen and carbon **3** are in closest proximity to the solvated lithium cation and predicted to have the greatest negative charges. In these examples, carbon **2** is more negative than carbon **1** and this is likely a result of the highly polarized bond between the ether oxygen and carbon **1**. In **3al-Li**, the bond distance from the lithium atom to carbon **1** is the longest (2.236 Å) in this coordination and cannot be explained based on the molecular orbital coefficients of the HOMO; however, this is consistent with the NPA charge analysis; O(-0.6), C1(-0.2), C2(-0.3), C3(-0.5). Carbon **3** is slightly closer to the lithium atom (2.121 Å) than carbons **1** or **2** which bends the allylic  $\pi$ -system out of the plane. The bond length between carbons **1** and **2** is 1.357 Å whereas the bond distance between the carbons **2** and **3** is 1.431 Å, suggesting that the  $\pi$ -bonding between carbons **2** and **3** is slightly less than that between carbons **1** and **2**. Bending the allylic  $\pi$ -system seems to relieve the steric strain caused by the butenyl terminal methyl group which is severely displaced out of the plane containing carbons **1** and **2** and away from the lithium atom in the optimized geometry. The geometries obtained for **4al-Li** and **8al-Li** are a result of several starting geometries designed to obtain a stationary point for each molecule with solvated lithium coordinating to the  $\pi$ -system of the allylic anion. However, as shown in Figure 3, the lowest energy conformers obtained for **4al-Li** and **8al-Li** do not include this feature. In the case of **8al-Li**, additional attempts at obtaining coordination to the ether oxygen of 2,3-dihydro-4H-pyran actually optimized to the structure shown in Figure 3. The coordination exhibited in the optimized geometry obtained for solvated allyl lithiated species **10al-Li** does not appear to follow either the HOMO coefficients or the charges obtained from NPA. Carbons **1** and **2** have similar charges (about -0.2 and -0.3 respectively), whereas carbon **3** and the ether oxygen have a charge value of about -0.6. The vinyl hydrogen and the three carbons (**1**, **2**, and **3**) in **10al-Li** are very nearly in the same plane; the dihedral angle is -182°.

The geometry obtained for **12al-Li** indicates coordination of solvated lithium to carbons **3**, **4**, and **5** of the pentadienyl anion and additionally to the ether oxygen of 2,3-dihydrooxepin. Both the molecular orbital coefficients of the HOMO and the charges for these atoms in the anion (**12al**) suggest that coordination should be at carbons **3** and **5**; the shorter bond length between the lithium atom and carbon **4** (2.228 Å) seems to be a consequence of coordination to the two adjacent carbons. Coordination of solvated lithium in **13al-Li** is consistent with the molecular orbital coefficients of the HOMO and the charges of the carbons **2**, **3**, and **4** in that carbon **3** has the most negative charge and the largest HOMO coefficients and is closest to the lithium atom.

**Angles of vinyl and allyl anions.** Optimized vinyl anions exhibit (Table 2) a vinyl angle

Table 2. Vinylic and Allylic Angles (°)

	Vinylic X - <sup>(-)</sup> C = C <u>Angle<sup>a</sup></u>	Allylic <sup>(-)</sup> C - C = C <u>Angle</u>		Vinylic X - <sup>(-)</sup> C = C <u>Angle<sup>a</sup></u>	Allylic <sup>(-)</sup> C - C = C <u>Angle</u>
<b>1</b>	123.3	125.8	<b>10</b>	127.2	127.6
<b>1v</b>	111.6	128.4	<b>10v</b>	116.2	132.2
<b>1al</b>	121.6	132.3	<b>10al</b>	121.8	129.6
<b>2</b>	123.3	126.1	<b>11</b>	126.5	126.5
<b>2v</b>	111.4	128.4	<b>11v</b>	115.6	128.6
<b>2al</b>	117.9	132.2	<b>11al</b>	124.7	132.2
<b>3</b>	125.4	131.1	<b>12</b>	129.0	125.9
<b>3v</b>	113.6	134.5	<b>12v</b>	117.8	123.7
<b>3al</b>	121.8	134.6	<b>12al</b>	126.3	128.7
<b>4</b>	98.9	86.4	<b>13</b>	128.7	128.7
<b>4v</b>	91.2	90.9	<b>13v</b>	117.4	128.3
<b>4al</b>	97.3	89.3	<b>13al</b>	125.8	131.2
<b>5</b>	94.5	94.5	<b>14</b>		
<b>5v</b>	88.0	99.5	<b>Boat</b>	121.2	123.4
<b>5al</b>	88.5	97.1	<b>14v</b>		
<b>6</b>	115.0	108.5	<b>Boat</b>	108.4	126.4
<b>6v</b>	106.3	113.1	<b>14al</b>		
<b>6al</b>	112.6	111.4	<b>Chair</b>	121.6	132.7
<b>7</b>	112.2	112.2	<b>15</b>		
<b>7v</b>	104.7	116.6	<b>Boat</b>	123.4	132.5
<b>7al</b>	105.6	114.0	<b>Chair</b>	124.2	126.9
<b>8</b>	125.1	122.1	<b>15v</b>		
<b>8v</b>	115.1	127.5	<b>Boat</b>	110.5	131.7
<b>8al</b>	118.6	124.5	<b>Chair</b>	110.3	125.9
<b>9</b>	123.6	123.6	<b>15al</b>		
<b>9v</b>	115.4	127.9	<b>Boat</b>	124.3	131.0
<b>9al</b>	118.4	126.1	<b>Chair</b>	125.8	138.6

<sup>a</sup> X=O,C

compression of about 7–13°. Calculations indicate that the vinyl angle in methoxyethene contracts about 15° upon vinyl deprotonation.<sup>28</sup> Optimized cyclic allyl anions exhibit an allyl angle expansion of about 1.8–11.7°. The boat conformation of **15**, however, exhibits an allylic angle compression of about 1.5° upon deprotonation at the allylic position to the anionic boat conformation (**15a1**). In the case of the chair conformation of **15a1**, the deprotonated carbon can freely donate its electrons to the neighboring conjugated  $\pi$ -system to form the resulting pentadienyl anion because the carbons comprising the pentadienyl anion are essentially coplanar. For the boat conformation of **15a1**, the dihedral angles describing the relative position of the five carbon atoms, that make up the pentadienyl anion in the chair conformer, are 23.9° and 16.4° and are clearly not coplanar. As a result, the allylic carbon, being the furthest out of the plane as compared to the other four carbons, has a difficult time donating electrons from its fully occupied p-orbital to the conjugated  $\pi$ -system and, as is seen with all of the vinyl anions, the fully occupied p-orbital of the allylic carbon (after deprotonation) repels the other substituents of the allylic carbon and has an overall effect of slightly compressing the ring at that carbon. The non-cyclic vinyl ethers **1**, **2**, and **3** exhibit an allylic angle expansion of 6.5°, 6.1°, and 3.5° respectively upon allylic deprotonation. This suggests that the allylic angle expansion (upon allylic deprotonation) is significantly hindered with the methyl group in the *syn* high energy conformation as in **3a1** as compared to the low energy conformation **2a1** which exhibits an allylic angle expansion of almost twice that of the higher energy conformer. Cyclic vinyl ethers, being structurally more similar to **3a1** than **2a1**, typically exhibit allylic angle expansions of 2°–2.9° and the cyclic vinyl hydrocarbons typically exhibit allylic angle expansions on the order of 1.8°–5.7° (Table 2). Upon vinyl deprotonation, vinyl angle compression generally increases with increasing ring size. With the exception of results obtained for **11** and **15**, the observed allylic angle expansion for the cyclic vinyl compounds is reasonably regular (about 2–3°) and does not seem to be significantly affected by ring size.

**Transition States.** In the application of complexation to allylic vs vinylic deprotonation of cyclic vinyl ethers, the focus is on the construction of transition states that illustrate the site-directed delivery of the alkyl anion mediated by lithium's initial coordination with an electron rich heteroatom; in this case oxygen. Figure 4 demonstrates a complexation mediated vinylic deprotonation reaction of **6** with methyl lithium involving an initial preequilibrium complexation going on to form the two possible transition states (**6v-ts** or **6al-ts**), which lose methane to form the unsolvated products **u-6v-Li** or **u-17-c** (respectively).

In Table 3, relative energies are reported corresponding to the progress of reaction for vinylic and allylic deprotonation of **8**, **10**, and **12**. Consistent with experimentally observed results for 2,3-dihydrofuran

Table 3. Progress of Reaction Relative Energies for Vinylic and Allylic Deprotonation of Cyclic Vinyl Ethers **8**, **10**, **12**

Computational Job	Parent + MeLi	Parent-MeLi Complex	Vinyl Transition State	Allyl Transition State	Vinyl Product + CH <sub>4</sub>	Allyl Product + CH <sub>4</sub>
RHF/6-31++G(d,p)//RHF/6-31++G(d,p)	<b>8</b> 0.0	<b>8c</b> -17.9	<b>8v-ts</b> 21.7	<b>8al-ts</b> 24.4	<b>u-8v-Li</b> -13.0	<b>u-8al-Li</b> -1.2
MP2/6-31++G(d,p)//RHF/6-31++G(d,p)	0.0	-18.9	8.9	5.2	-15.1	-6.7
RHF/6-31++G(d,p)//RHF/6-31++G(d,p)	<b>10</b> 0.0	<b>10c</b> -18.8	<b>10v-ts</b> 22.0	<b>10al-ts</b> 18.8	<b>u-10v-Li</b> -12.0	<b>u-10al-Li</b> -12.9
MP2/6-31++G(d,p)//RHF/6-31++G(d,p)	0.0	-20.0	7.9	0.6	-15.3	-21.0
RHF/6-31++G(d,p)//RHF/6-31++G(d,p)	<b>12</b> 0.0	<b>12c</b> -16.9	<b>12v-ts</b> 21.9	<b>12al-ts</b> 15.9	<b>u-12v-Li</b> -13.2	<b>u-12al-Li</b> -25.6
MP2/6-31++G(d,p)//RHF/6-31++G(d,p)	0.0	-17.8	8.6	2.3	-15.4	-35.1

(6, Figure 4), the transition state presumably responsible for vinyl deprotonation (**6v-ts**) is about 7 kcal/mol (HF) and 1 kcal/mol (MP2) lower in energy than the transition state located for allylic deprotonation (**6al-ts**) and, in addition, the *unsolvated* vinyl lithiated species **6v-Li** (**u-6v-Li**) is about 9 kcal/mol (HF) and 3 kcal/mol (MP2) lower in energy than the unsolvated allyl lithiated species **u-6al-Li** using the 6-31++G(d,p) basis set. For 2,3-dihydro-4H-pyran (**8**), relative energies obtained at the Hartree-Fock level of theory, concordant with the experimentally observed product (**u-8v-Li**), suggest that the transition state corresponding to vinylic deprotonation (**8v-ts**) is about 3 kcal/mol lower in energy than the transition state corresponding to allylic deprotonation (**8al-ts**). Single point energies obtained with second-order Møller Plesset perturbation theory with precisely the same geometries predict **8v-ts** to be 4 kcal/mol higher in energy than **8al-ts**. With regard to the vinyl and allyl lithiated products (**u-8v-Li**, **u-8al-Li** respectively), calculations at both levels of theory suggest **u-8v-Li** to be lower in energy than **u-8al-Li** by about 12 kcal/mol (HF) and 8 kcal/mol (MP2). The transition state **10v-ts**, corresponding to vinylic deprotonation of 2,3,4,5-tetrahydrooxepin, is predicted to be less stable by about 3

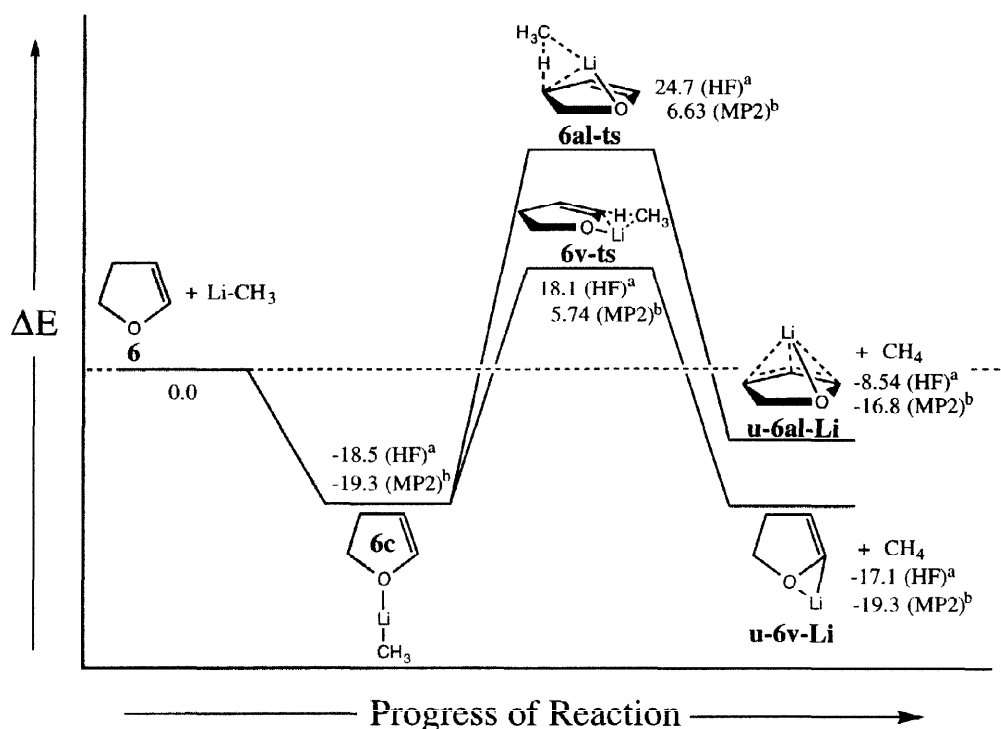


Figure 4. Progress of Reaction Diagram for Formation of Vinyl and Allyl Lithiated Species  
**u-6v-Li and u-6al-Li** (Energies are in kcal/mol)

<sup>a</sup> RHF/6-31++G(d,p)//RHF/6-31++G(d,p). <sup>b</sup> MP2/6-31++G(d,p)//RHF/6-31++G(d,p)

kcal/mol (HF) and 7 kcal/mol (MP2) than the transition state located for allylic deprotonation (**10al-ts**). Also the vinyl lithiated species **u-10v-Li** is about 1 kcal/mol (HF) and 6 kcal/mol (MP2) higher in energy than the allyl lithiated species **u-10al-Li**. Unfortunately, all of these observations would lead one to believe, contradictory to the experimental results, that the allyl lithiated species should be experimentally observed, not the vinyl lithiated species. Relative energies obtained at both levels of theory with the 6-31++G(d,p) basis set for 2,3-dihydrooxepin (**12**), and in accord with experimental observations, indicate that the transition state located for vinylic deprotonation (**12v-ts**) is 6 kcal/mol (HF and MP2) higher in energy than the transition state presumably responsible for allylic deprotonation (**12al-ts**) and, in addition, the vinyl lithiated species **u-12v-Li** is 12 kcal/mol (HF) and 20 kcal/mol (MP2) higher in energy than the allyl lithiated product **u-12al-Li**, which collapses to the experimentally observed product (1-lithio-1-oxoheptatriene). The difference in relative energies between the solvated species corresponding to vinylic and allylic lithiation (Table 1) are strikingly similar (both qualitatively and quantitatively) to that of the corresponding unsolvated species (Table 3) for all but one example. At the Hartree-Fock level of theory, the solvated vinyl lithiated species **10v-Li** is lower in energy than the solvated allyl lithiated species **10al-Li** by about 1 kcal/mol whereas the unsolvated vinyl lithiated species **u-10v-Li** is predicted to be about 1 kcal/mol higher in

energy than the unsolvated allyl lithiated species **u-10al-Li**. Relative energies obtained at the Hartree-Fock level of theory for all of the transition states listed in Figure 4, Table 3 are overestimated as compared to those obtained employing second-order Møller Plesset perturbation theory.

Employing the 6-31++G(d,p) basis set to optimize the model transition states at the Hartree-Fock level of theory, as well as calculating MP2 single-point energies associated with these optimized geometries, in order to gain insight into vinylic vs allylic deprotonation reactions of cyclic vinyl ethers with organolithium reagents is not completely successful with respect to experimental observations (Table 3). Although the model transition states can be used to explain the cases of 2,3-dihydrofuran and 2,3-dihydrooxepin, the computational results for transition states **8v-ts** vs **8al-ts** at the MP2 level for 2,3-dihydro-4H-pyran are inconsistent with results at the Hartree-Fock level of theory; and it is the Hartree-Fock relative energies that agree with experimental results. Additionally, the computational results for 2,3,4,5-tetrahydrooxepin with respect to both the transition states and the lithiated species are not consistent with experimental results at either level of theory. In an attempt to address these discrepancies, we employed the Density Functional Method B3LYP to calculate single-point energies and additionally, we reoptimized **8v-ts** and **8al-ts** at the Hartree-Fock level of theory using basis set 6-311++G(d,p) (Table 4). We note that Kremer et al.<sup>29</sup> utilized the B3LYP-DFT method and the 6-311++G(d,p) basis set for similar types of transition state calculations and this was certainly one of our major reasons for the incorporation of

Table 4. Additional Relative Energies (kcal/mol) of Transition States Corresponding to Vinylic and Allylic Deprotonation of **8** and **10**

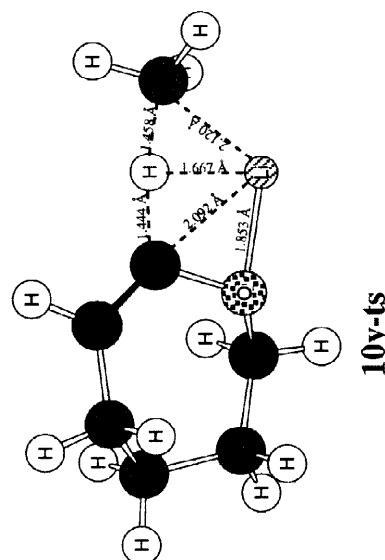
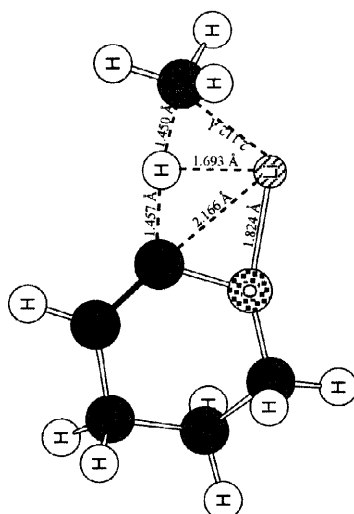
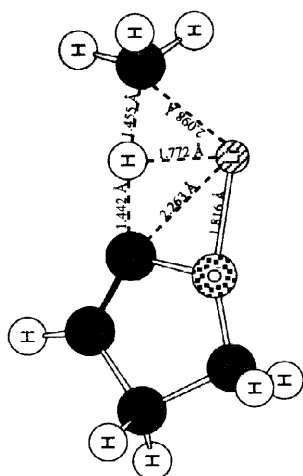
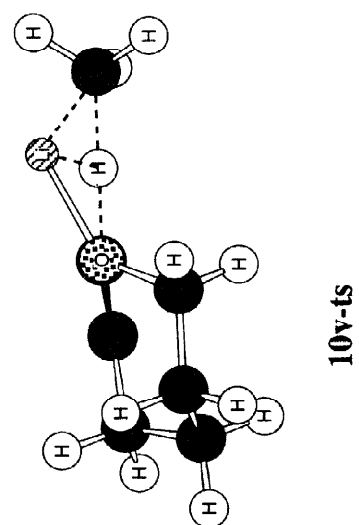
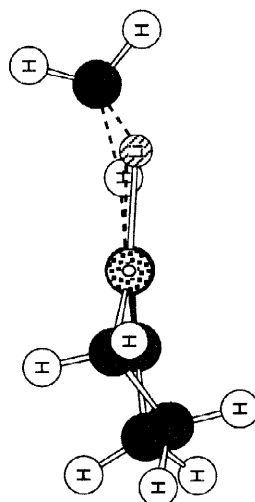
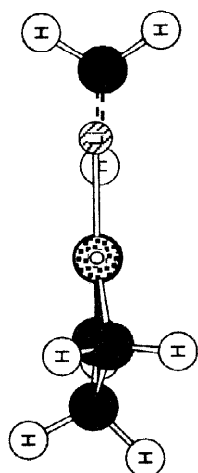
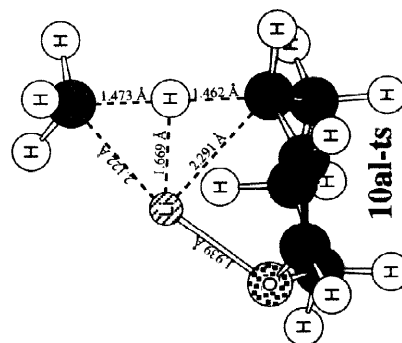
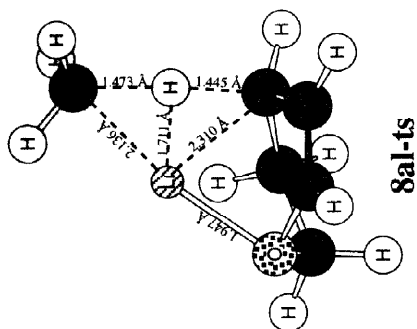
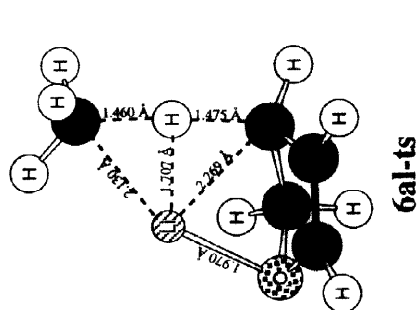
Computational Job	Vinyl Transition State	Allyl Transition State
	<b>8v-ts</b>	<b>8al-ts</b>
B3LYP/6-31++G(d,p)//RHF/6-31++G(d,p)	2.6	0.0
RHF/6-311++G(d,p)//RHF/6-311++G(d,p)	0.0	3.0
B3LYP/6-311++G(d,p)//RHF/6-311++G(d,p)	2.5	0.0
MP2/6-311++G(d,p)//RHF/6-311++G(d,p)	4.3	0.0
	<b>10v-ts</b>	<b>10al-ts</b>
B3LYP/6-31++G(d,p)//RHF/6-31++G(d,p)	6.2	0.0
RHF/aug-cc-pVDZ (H,C,O) 6-31G (Li)		
//RHF/aug-cc-pVDZ (H,C,O) 6-31G (Li)	3.6	0.0

them into our work here. Qualitatively, the B3LYP/6-31++G(d,p)//RHF/6-31++G(d,p) relative energies are in agreement with those obtained from the MP2/6-31++G(d,p)//RHF/6-31++G(d,p) single point calculations, showing that **8al-ts** is lower in energy than **8v-ts** by about 3 kcal/mol. Relative energies obtained from the Hartree-Fock optimizations and DFT and MP2 single point calculations with the 6-311++G(d,p) basis set are very similar to those obtained with the 6-31++G(d,p) basis set. Also the geometries associated with these stationary points are quite similar to those obtained with 6-31++G(d,p). In Table 4, we present B3LYP single point energies obtained with the 6-31++G(d,p) basis set for **10v-ts** and **10al-ts** using the geometries obtained from a Hartree-Fock optimization (Table 3). As was the case, for **8v-ts** vs. **8al-ts**, these relative energies are qualitatively similar to results obtained from second-order Møller Plesset perturbation theory (Table 3). As a point of comparison, we performed a Hartree-Fock optimization of **10v-ts** and **10al-ts** with the aug-cc-pVDZ (H,C,O) as well as 6-31G (Li) and, for all practical applications, we recognize this to be the limit of our current computational resources. The Hartree-Fock relative energies obtained with this basis set suggest **10v-ts** to be about 3.6 kcal/mol higher in energy than **10al-ts**. These results are quite similar to those obtained at this level of theory with the much smaller 6-31++G(d,p) basis set and serve to demonstrate that deviations from experimental observations are not likely caused by basis set deficiencies but rather, among other considerations, deficiencies in the model transition states in this study.

**Transition State Structures.** The geometries located for transition states **6v-ts**, **6al-ts**, **8v-ts**, **8al-ts**, **10v-ts**, **10al-ts**, **12v-ts**, and **12al-ts** from RHF/6-31++G(d,p)//RHF/6-31++G(d,p) are presented in Figure 5 along with specific bond lengths (in Å) associated with the deprotonation reaction. The transition states corresponding to vinylic deprotonation are pictured twice; on the left, the Chem 3D geometry is drawn so that the lithium complex region is approximately coplanar with the paper, and the structure on the right is a 90° rotation of the left view. As the ring size increases from **6v-ts** to **12v-ts**, the transition states corresponding to vinyl deprotonation become less and less planar. The geometries for all of the transition states suggest that the complexation mediated deprotonation reactions involving organolithium reagents occur in a concerted fashion and not step-wise, precluding the formation of an anion. This suggests that the relative stabilities of the corresponding anions (Table 1) have little (or nothing) to do with the observed lithiated species. The departing methyl group is approximately the same distance from lithium as the carbon being deprotonated.

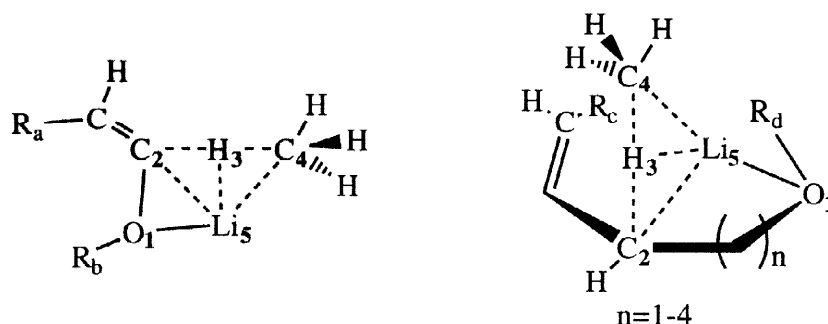
**Unsolvated Structures.** With the exception of **u-8al-Li**, the coordination of a lithium cation to vinyl ethers is very much the same as the coordination seen with a solvated lithium cation (Figure 3).





**Charges Analyses.** Recently Kremer, Junge, and Schleyer<sup>29</sup> reported transition states corresponding to side-chain directed metallation of ortho-substituted toluenes using lithium hydride in their model transition states. These transition states are strikingly similar to those in Figure 5. In order to further characterize the transition states in Figure 5, as was done by Kremer et al.,<sup>29</sup> the atomic charges were determined from a Natural Population Analysis (NPA),<sup>26-27</sup> using the MP2 electron density (Table 5).

Table 5. NPA Charges Calculated for Transition States (Figure 5)  
 Invoking Complexation Mediated Vinylic and Allylic Deprotonation



		NPA			NPA
<b>6v-ts</b>	O <sub>1</sub>	-0.705	<b>6al-ts</b>	O <sub>1</sub>	-0.636
	C <sub>2</sub>	-0.039		C <sub>2</sub>	-0.662
	H <sub>3</sub>	0.227		H <sub>3</sub>	0.210
	C <sub>4</sub>	-1.216		C <sub>4</sub>	-1.163
	Li <sub>5</sub>	0.934		Li <sub>5</sub>	0.899
<b>8v-ts</b>	O <sub>1</sub>	-0.692	<b>8al-ts</b>	O <sub>1</sub>	-0.652
	C <sub>2</sub>	-0.064		C <sub>2</sub>	-0.632
	H <sub>3</sub>	0.213		H <sub>3</sub>	0.215
	C <sub>4</sub>	-1.203		C <sub>4</sub>	-1.150
	Li <sub>5</sub>	0.931		Li <sub>5</sub>	0.891
<b>10v-ts</b>	O <sub>1</sub>	-0.709	<b>10al-ts</b>	O <sub>1</sub>	-0.665
	C <sub>2</sub>	-0.091		C <sub>2</sub>	-0.656
	H <sub>3</sub>	0.210		H <sub>3</sub>	0.209
	C <sub>4</sub>	-1.201		C <sub>4</sub>	-1.162
	Li <sub>5</sub>	0.930		Li <sub>5</sub>	0.900
<b>12v-ts</b>	O <sub>1</sub>	-0.686	<b>12al-ts</b>	O <sub>1</sub>	-0.653
	C <sub>2</sub>	-0.036		C <sub>2</sub>	-0.648
	H <sub>3</sub>	0.208		H <sub>3</sub>	0.215
	C <sub>4</sub>	-1.204		C <sub>4</sub>	-1.169
	Li <sub>5</sub>	0.931		Li <sub>5</sub>	0.911

R<sub>a</sub>=H, alkyl, alkenyl; R<sub>b</sub>=H, alkyl, alkenyl

R<sub>c</sub>=ether, alkenyl ether; R<sub>d</sub>=vinyl

Examination of the charges of the migrating hydrogens indicates that the charge on hydrogen is low for every transition state in Figure 5. The arrangement of charges suggests that the transition states are multi-center processes.

## CONCLUSIONS

With two exceptions, computational analysis of the relative stabilities of vinyl and allyl anions is in good agreement with the experimentally observed vinyl and allyl lithiated products. In the case of 2,3-dihydro-4H-pyran and 2,3,4,5-tetrahydrooxepin, the computational results for the anions suggest that the experimentally observed vinyl lithiated species result from the preceding higher energy vinyl anions (Table 1). Although relative anion stability may have something to do with vinyl vs allyl lithiation, it clearly is not the only contributor directing the observed products of this reaction. For cyclic vinyl ethers, a general trend can be drawn from the computational results presented where the stability of the allylic anion over the vinylic anion in terms of ring size is  $8 \approx 7 > 6 > 5 \approx 4$ . A similar trend for the cyclic alkenes can also be made. Generally speaking, optimized vinyl anions exhibit a vinyl angle compression and optimized allyl anions exhibit an allyl angle expansion. Vinylic vs allylic deprotonation reactions involving vinyl ethers and organolithium reagents may proceed through transition states via complexation. With 2,3,4,5-tetrahydrooxepin, the relative energies of the transition states and lithiated products are not consistent with the experimentally observed vinyl lithiated species (Table 3). The transition state geometries and atomic charges obtained in the present study depict multicenter processes involving coordination of lithium to the vinyl ether oxygen, departing proton, vinyl (or allyl) anion, and the departing methyl carbon.

SCF treatment of geometry optimizations of these types of structures to obtain reliable geometries and relative energies may very well introduce short-comings to our present work; inclusion of MP2 single-point energies is not equivalent to geometry optimizations at this level of theory but they do suggest how inclusion of electron correlation may affect relative energies. The choice of not including aggregation in this study to explain the vinylic and allylic deprotonation reactions is an attempt at modeling these types of reactions at the simplest practical level for these rather large compounds. Solvation of lithium may be important in these reactions and no attempt has been made here to include solvation effects in our transition state studies. Significant improvements to the level of theory studied will require a major increase in computational resources and this is an obstacle we can not overcome at the present time.

**ACKNOWLEDGMENT:** We would like to thank Dr. S. Mark Cybulski for his many generous hours of assistance with Gaussian 94 and the SGI and, in addition, we are appreciative of his constructive criticisms during the writing of this manuscript. We are grateful for helpful communications with Dr. Alice Chung-Phillips concerning the NPA method. Additionally, we appreciate the advice given by Dr. Kui Zhang regarding the location of transition states. We would like to acknowledge the NSF Grant # DUE-9551091 used for the purchase of the Silicon Graphics Power Indigo (SGI) workstation and Gaussian 94.

Computations were supported , in part, by the Ohio Board of Regents Separation Science Consortium (RS/6000).

### REFERENCES

1. Oakes, F. T.; Sebastian, J. F. *J. Org. Chem.* **1980**, *45*, 4959-4961.
2. Oakes, F. T.; Yang F-A; Sebastian, J. F. *J. Org. Chem.* **1982**, *47*, 3094-3097.
3. Recently we reported preliminary results:  
Power, T. D.; Sebastian, J. F. *Tetrahedron Lett.* **1996**, *37*, 9127-9130.
4. Harris, N. J.; Sebastian, J. F. *Tetrahedron Lett.* **1991**, *32*, 6069-6072.
5. Bauer, W.; Schleyer, P. v.R. *J. Am. Chem. Soc.* **1989**, *111*, 7191-7198.
6. Bachrach, S. M.; Ritchie, J. P. *J. Am. Chem. Soc.* **1989**, *111*, 3134-3140.
7. Stork, G.; Polt, R. L.; Li, Y.; Houk, K. N. *J. Am. Chem. Soc.* **1988**, *110*, 8360-8367.
8. Beak, P.; Meyers, A. I. *Acc. Chem. Res.* **1986**, *19*, 356-363.
9. Beak, P.; Hunter, J. E.; Jun, Y. M. *J Am Chem Soc.* **1983**, *105*, 6350-6351.
10. Gaussian 94, Revision B.3, Frisch, M. J.; Trucks, G. W.; Schlegel, H. B.; Gill, P. M. W.; Johnson, B. G.; Robb, M. A.; Cheeseman, J. R.; Keith, T.; Petersson, G. A.; Montgomery, J. A.; Raghavachari, K.; Al-Laham, M. A.; Zakrzewski, V. G.; Ortiz, J. V.; Foresman, J. B.; Peng, C. Y.; Ayala, P. Y.; Chen, W.; Wong, M. W.; Andres, J. L.; Replogle, E. S.; Gomperts, R.; Martin, R. L.; Fox, D. J.; Binkley, J. S.; Defrees, D. J.; Baker, J.; Stewart, J. P.; Head-Gordon, M.; Gonzalez, C.; and Pople, J. A. Gaussian, Inc., Pittsburgh PA, 1995.
11. Dunning, T. H., Jr. *J. Chem. Phys.* **1989**, *90*, 1007-1023.
12. Woon, D. E.; Dunning, T. H., Jr. *J. Chem. Phys.* **1994**, *100*, 2975-2988.
13. Kendall, R. A.; Dunning, T. H., Jr.; Harrison, R. J. *J. Chem. Phys.* **1992**, *96*, 6796-6806.
14. Woon, D. E.; Dunning, T. H., Jr. *J. Chem. Phys.* **1993**, *98*, 1358-1371.
15. Woon, D. E.; Dunning, T. H., Jr. *J. Chem. Phys.* **1995**, *103*, 4572-4585.
16. Becke, A. D. *J. Chem. Phys.* **1993**, *98*, 5648-5652.
17. Becke, A. D. *Phys. Rev. A* **1988**, *38*, 3098-3100.
18. Lee, C.; Yang, W.; Parr, R. G. *Phys. Rev. B* **1988**, *37*, 785-789.
19. Vosko, S. H.; Nusair, M. *Can. J. Phys.* **1980**, *58*, 1200-1211.
20. Allen, F. H. *Acta Crystallogr., Sect. B: Struct. Sci.* **1984**, *B40(1)*, 64-72.
21. Bak, B.; Led, J. J.; Nygaard, L.; Rastrup-Andersen, J.; Sørensen, G. O. *J. Mol. Struct.* **1969**, *3*, 369-378.
22. Davis, M. I.; Muecke, T. W. *J. Phys. Chem.*, **1970**, *74(5)*, 1104-1108.

23. Chiang, J. F.; Bauer, S. H. *J. Am. Chem. Soc.* **1969**, *91*, 1898-1901.
24. Ermolaeva, L. I.; Mastryukov, V. S.; Allinger, N. L.; Almenningen, A. *J. Mol. Struct.* **1989**, *196*, 151-156.
25. Hagen, K.; Trætteberg, M. *Acta Chem. Scand.* **1972**, *29(9)*, 3643-3648.
26. Reed, A. E.; Weinstock, R. B.; Weinhold, F. *J. Chem. Phys.* **1985**, *83*, 735-746.
27. Reed, A. E.; Curtiss, L. A.; Weinhold, F. *Chem. Rev.* **1988**, *88*, 899-926.
28. Rossi, A. R.; Remillard, B. D.; Gould, S. J. *Tetrahedron Lett.* **1978**, 4357-4360.
29. Kremer, T.; Junge, M.; Schleyer, P. v.R. *Organometallics* **1996**, *15*, 3345-3359.
30. Goldfuss, B.; Schleyer, P. v.R.; Hampel, F. *J. Am. Chem. Soc.* **1996**, *118*, 12183-12189.
31. Hommes, N. J. R. v.E.; Schleyer, P. v.R. *Tetrahedron* **1994**, *50*, 5903-5916.
32. Goldfuss, B.; Schleyer, P. v.R.; Hampel, F. *J. Am. Chem. Soc.* **1997**, *119*, 1072-1080.
33. Bauer, W.; O'Doherty, G. A.; Schleyer, P. v.R.; Paquette, L. A. *J. Am. Chem. Soc.* **1991**, *113*, 7093-7100.
34. Sorger, K.; Schleyer, P. v.R.; Fleischer, R.; Stalke, D. *J. Am. Chem. Soc.* **1996**, *118*, 6924-6933.
35. Bolton, E. E.; Laidig, W. D.; Schleyer, P. v.R.; Schaefer, H. F. III *J. Phys. Chem.* **1995**, *99*, 17551-17557.
36. Armstrong, D. R.; Barr, D.; Raithby, P. R.; Snaith, R.; Wright, D. S.; Schleyer, P. v.R. *Inorg. Chim. Acta* **1991**, *185*, 163-167.
37. Barr, D.; Raithby, P. R.; Schleyer, P. v.R.; Snaith, R.; Wright, D. S. *J. Chem. Soc., Chem. Commun.* **1990**, *8*, 643-645.
38. Kremer, T.; Schleyer, P. v.R. *Organometallics* **1997**, *16*, 737-746.